Available online at www.sciencedirect.com
ScienceDirect
Polymer 49 (2008) 792–799
polymer
www.elsevier.com/locate/polymer

Anisotropy of the modulus of elasticity in regenerated cellulose fibres related to molecular orientation

W. Gindl [a,b,*], M. Reifferscheid [a], R.-B. Adusumalli [b], H. Weber [b], T. Röder [c], H. Sixta [b,c], T. Schöberl [d]

[a] *Department of Materials Science and Process Engineering, BOKU, Vienna, Austria*
[b] *Kompetenzzentrum Holz GmbH, Linz, Austria*
[c] *Lenzing AG, Lenzing, Austria*
[d] *Erich Schmid Institute for Materials Science, Austrian Academy of Sciences, Leoben, Austria*

Received 28 August 2007; received in revised form 22 November 2007; accepted 17 December 2007
Available online 23 December 2007

Abstract

Regenerated cellulose fibres of different origin were tested in tension and by means of nanoindentation. Their degree of molecular orientation was characterised with birefringence measurements. An empirical relationship was set up between the degree of orientation expressed by birefringence and the modulus of elasticity parallel to the fibre direction, and the ratio between this modulus and the modulus transverse to the fibre direction, respectively.

Keywords: Anisotropy; Molecular orientation; Regenerated cellulose fibres

1. Introduction

Regenerated cellulose fibres [1], which are produced by the dissolution of purified cellulose from, mostly woody, biomass in a suitable solvent and subsequent spinning, own a significant share of the textile fibre market. The widely used viscose process involves the treatment of cellulose with sodium hydroxide and carbon disulfide before it is spun into an acidic precipitation bath. High-tenacity rayon fibres produced by a modification of the classic viscose process find application as reinforcement fibres in car tires. The more recently developed environmentally friendly lyocell process is based on the direct dissolution of cellulose in a mixture of water and *N*-methylmorpholine-*N*-oxide without derivatisation. Lyocell fibres are currently used in textiles and nonwovens. Apart from these classical applications, the success of natural cellulose fibres such as flax, kenaf, and hemp in the reinforcement of polymer composites [2] has spurred considerable interest in the suitability of regenerated cellulose fibres for polymer reinforcement [3–7]. Finally, regenerated cellulose fibres are also of interest with regard to serving as precursor in the production of carbon fibres [8,9]. When comparing lyocell and rayon, carbon fibres produced from lyocell precursor show significantly improved properties compared to those produced from rayon precursor [10,11].

Particularly, with regard to the non-textile use of regenerated cellulose fibres, their strength and stiffness, which can be tuned within a wide range in the production process, is of high importance. The relationship between the molecular and supramolecular structures of regenerated cellulose fibres and their mechanical properties in the direction of the fibre axis has been extensively studied (e.g., see Ref. [12–16]). In the case of well-oriented cellulose fibres, the fibre compliance is related to the orientation parameter $\langle \sin^2 \Phi \rangle_E$ by Eq. (1)

* Corresponding author. Department of Materials Science and Process Engineering, BOKU-Vienna, Vienna, Austria. Tel.: +43 1 47654 4255; fax: +43 1 47654 4295.
E-mail address: wolfgang.gindl@boku.ac.at (W. Gindl).

0032-3861/$ - see front matter © 2007 Elsevier Ltd. All rights reserved.
doi:10.1016/j.polymer.2007.12.016

$$\frac{1}{E}=\frac{1}{e_c}+\frac{\langle \sin^2 \Phi \rangle_E}{2g} \quad (1)$$

where E is the modulus of elasticity in fibre direction, e_c is the chain modulus and g is the average shear modulus between adjacent chains [17,18]. It is noted for clarity that throughout this paper capital letters (E and G) are used to denote macroscopic moduli, whereas moduli for the cellulose chain (e and g) are given in lower case. The strain orientation parameter $\langle \sin^2 \Phi \rangle_E$ represents the average orientation of all polymer chains at zero strain. This orientation parameter is equivalent to the orientation parameter $\langle \sin^2 \theta \rangle$ (Eq. (2)), which is the second moment of the molecular orientation distribution [19], only in well-oriented fibres with a Gaussian distribution of chain orientation [20].

$$\langle \sin^2 \theta \rangle = \frac{2}{3}\left(1-\frac{\Delta n}{\Delta n_{max}}\right) \quad (2)$$

In Eq. (2), Δn is the measured birefringence and Δn_{max} is the maximum birefringence of cellulose. The validity of the model shown in Eq. (1) for well-oriented regenerated cellulose fibres was confirmed recently [21]. However, in order to fully understand the behaviour of cellulose fibre reinforcement in polymer composites, it is also necessary to study mechanical fibre properties transverse to the fibre direction.

In the present study, we chose two different approaches to study the changing ratio of the modulus of elasticity of regenerated cellulose fibres parallel and transverse to the fibre direction, respectively, independent of their degree of preferred molecular orientation. First, a high number of regenerated cellulose fibres and few cellulose films, covering a broad range of preferred orientation, were tested in tension and preferred orientation was determined by means of birefringence measurements. By fitting an empirical mathematical relationship to these experimental data, the modulus of elasticity transverse to the direction of the cellulose chain can be inferred, and an estimate of the anisotropy (i.e. the ratio of the modulus of elasticity parallel and transverse to the fibre direction) of a regenerated cellulose fibre can be made from the degree of preferred orientation of its constituent cellulose chains. In a second approach, direct measurements of the modulus of elasticity of cellulose fibres parallel and transverse to the fibre direction were undertaken by means of nanoindentation technique and the fibre anisotropy was calculated from these measurements. The results of both approaches are compared and an assessment of their respective validity is made.

2. Materials and methods

Viscose and lyocell fibres were obtained from Lenzing R&D, Lenzing, Austria. Viscose fibres were received as staple fibres with a length of 38 mm. The four different lyocell fibres selected for this study were produced from the same spinning dope and differed only in the draw which was applied during production, resulting in different diameter and, consequently, different structural ad mechanical properties. Bocell fibres were kindly supplied by Dr. S. J. Eichhorn, University of Manchester, UK. These high-modulus/high-strength experimental fibres spun from an anisotropic solution in phosphoric acid owe their outstanding mechanical properties to exceptionally high crystallinity and high molecular orientation as described in detail by Northolt et al. [20] and Eichhorn et al. [16]. Regenerated cellulose films were prepared by dissolution of lyocell fibres in lithium chloride/*N*,*N*-dimethylacetamide solvent and subsequent casting as described in detail in Ref. [22]. The thickness of these films was between 0.1 mm and 0.2 mm. While one set of films was tested as produced, a second set was subjected to a uniaxial stretching procedure in order to introduce preferred orientation. Square pieces of cellulose film with a size of 50 mm × 50 mm were submerged in distilled water until saturation and subsequently fixed to the grips of a Zwick 20 kN universal testing machine. The films were stretched to a strain of 50% in wet condition and left to dry in the stretched state, thus preserving the obtained preferred orientation [22].

2.1. Characterisation of molecular orientation

The degree of preferred orientation in cellulose fibres and films was determined by means of birefringence measurements. A Zeiss Axioimager microscope equipped with a Berek compensator 5λ was used. The birefringence Δn of a specimen was obtained by dividing the measured retardation of polarised light by the respective specimen thickness. By relating Δn to the maximum birefringence of cellulose Δn_{max}, the orientation factor f (Hermans' orientation factor) was calculated according to Eq. (3).

$$f=\frac{\Delta n}{\Delta n_{max}} \quad (3)$$

Hermans' orientation factor is 1 for perfect orientation parallel to the fibre direction, 0 for random orientation, and −1 for perfect transverse orientation. While this procedure is straightforward for cellulose fibres, two birefringence values at an angle of 90° to each other were measured for cellulose films transverse to the direction of loading. A representative value of birefringence was estimated from these measurements by calculating an average value.

2.2. Determination of Poisson's ratio

Poisson's ratio was determined for the cellulose II crystallite [23]. It was found to vary between 0.30 for the 200/004 plane and 0.46 for the 110/004 plane. For the $1\bar{1}0/004$ plane, a negative Poisson's ratio of −0.37 was calculated. Since it is difficult to derive a representative Poisson's ratio for bulk cellulose specimens from these values, own measurements were performed using unoriented cellulose films. The films were fixed to the grips of a universal testing machine and strained. During straining, the deformation of the specimen was monitored by means of an electronic laser speckle interferometer system (ESPI, Dantec-Ettemaier). By differentiation of the obtained

Table 1
Average diameter, mechanical properties, and degree of orientation of different kinds of regenerated cellulose fibres

Fibre	d	E (GPa)	σ_{max} (MPa)	ε_{max} (%)	$E_{l\text{-}NI}$ (GPa)	$E_{t\text{-}NI}$ (GPa)	Δn	f
Bocell	11.6	46.6 ± 6.5	1170 ± 165	6.1 ± 0.8	18.2 ± 1.7	6.7 ± 0.3	0.0536 ± 0.0035	0.87 ± 0.057
Lyocell A	9.0	31.2 ± 1.5	624 ± 58	6.8 ± 1.7	17.5 ± 0.8	4.9 ± 0.2	0.0449 ± 0.0003	0.73 ± 0.005
Lyocell B	10.5	30.3 ± 2.2	621 ± 57	7.5 ± 1.8	17.4 ± 0.7	4.9 ± 0.3	0.0446 ± 0.0004	0.72 ± 0.006
Lyocell C	17.3	27.3 ± 2.0	551 ± 27	9.8 ± 1.4	14.6 ± 0.8	5.0 ± 0.3	0.0430 ± 0.0003	0.70 ± 0.005
Lyocell D	26.5	22.4 ± 1.5	472 ± 29	13.7 ± 1.7	14.2 ± 0.8	5.8 ± 0.3	0.0397 ± 0.0002	0.64 ± 0.003
Viscose	10.5	11.5 ± 2.0	423 ± 48	19.0 ± 2.7	9.2 ± 0.6	6.1 ± 0.3	0.0247 ± 0.0029	0.40 ± 0.047

d: diameter; E: modulus of elasticity in fibre direction measured in a tensile test; σ_{max}: tensile strength; ε_{max}: elongation at break; $E_{l\text{-}NI}$: modulus of elasticity in fibre direction measured by nanoindentation; $E_{t\text{-}NI}$: modulus of elasticity transverse to the fibre direction measured by nanoindentation; Δn: birefringence; f: Hermans' orientation parameter.

displacement maps, the strains parallel and transverse to the direction of loading were obtained and Poisson's ratio was calculated. A detailed description of the method may be found in Ref. [24]. The value obtained from these measurements covers both crystalline and amorphous cellulose at random orientation and is therefore presumed suitable for further calculations.

2.3. Tensile testing

The cellulose fibres were fixed to paper frames with a free length of 30 mm as described in detail in Ref. [25] and tested until failure at a speed of 1 mm min^{-1}. For the mechanical characterisation of cellulose films, strips with a width of 5 mm and a length of 50 mm were cut. In the case of those films, which were stretched to introduce preferred orientation, the strips for tensile testing were cut with their length transverse to the direction of stretching, in order to obtain data points for cellulose with preferred orientation transverse to the direction of straining and thus very low modulus. While the calculation of strain from the tested free length and the recorded machine cross-head displacement is sufficiently accurate for cellulose fibres [25], direct deformation measurement was performed for all tested cellulose films using Zwick Macrosence clip-on displacement sensors.

2.4. Nanoindentation

In order to provide a second, independent data set on the mechanical properties of cellulose fibres with varying degree of preferred orientation, nanoindentation measurements were performed parallel and transverse to the fibre direction. For this purpose, fibres were embedded in epoxy resin and a smooth surface was cut by means of an ultramicrotome equipped with a diamond knife. Before performing nanoindentation, the fibres were imaged with an AFM (Digital Instruments DI Dimension 3100). From the AFM data, the diameter of the fibre was determined and the surface roughness of the specimens was evaluated. The average surface roughness was less than 2 nm, which is considered by far sufficiently smooth for our nanoindentation experiments. Using a Hysitron Triboscope indentation device, measurements were performed in a force-controlled mode with a Berkovich-type triangular diamond pyramid, applying a peak force of 140 μN. The elastic modulus was evaluated according to Oliver and Pharr [26].

3. Results

3.1. Molecular orientation

The materials selected for this study show a high variability in birefringence as shown in Tables 1 and 2. In order to calculate the average molecular orientation from birefringence measurements, the value of maximum birefringence in the case of perfect orientation of all cellulose chains parallel to the fibre direction has to be known. An evaluation of the maximum birefringence can be made by plotting the fibre birefringence against fibre compliance for well-oriented fibres (compliance < 0.04, [27]). When the compliance of the cellulose chain is known, the maximum birefringence can be derived by fitting a linear regression to the plotted data (Fig. 1). In the present study, the compliance of the cellulose chain was assumed to be 1/88 GPa^{-1} as calculated by Nishino et al. [28]. Based on these assumptions, a value of 0.0615 was obtained for maximum birefringence (Fig. 1), and used thereafter for the calculation of Hermans' orientation factor f according to Eq. (3). As seen in Tables 1 and 2, a large part of the theoretical range of f from 1 at perfectly longitudinal to −1 at perfectly transverse orientation is covered by experimental data obtained in the present study, providing a good basis for further analysis.

3.2. Mechanical properties by tensile testing

Typical stress–strain curves and average values of the modulus of elasticity, the tensile strength, and the elongation at break of a wide range of regenerated cellulose fibres are shown in Fig. 2 and in Table 1. The highest modulus and strength

Table 2
Mechanical properties, and degree of orientation of an unstretched and a stretched regenerated cellulose films tested in tension transverse to the direction of stretching

	E (GPa)	σ_{max} (MPa)	ε_{max} (%)	Δn	f
Unstretched film	8.5 ± 1.6	149 ± 7	11.6 ± 1.4	0.0089 ± 0.0003	0.14 ± 0.005
Stretched film	4.1 ± 0.5	62 ± 8	10.9 ± 3.3	−0.0262 ± 0.0006	−0.42 ± 0.009

E: modulus of elasticity; σ_{max}: tensile strength; ε_{max}: elongation at break; Δn: birefringence; f: Hermans' orientation parameter.

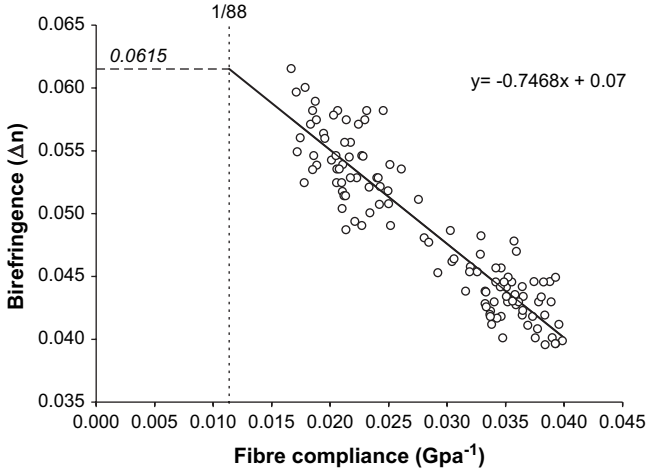

Fig. 1. Relationship between the compliance ($1/E$) of well-oriented regenerated cellulose fibres and their birefringence. By fitting a linear regression, the maximum birefringence of regenerated cellulose is obtained at the intercept of the fitted line (full line) and the compliance of a cellulose II chain (1/88 Gpa, dashed line). The equation of the line fitted by linear regression is also given.

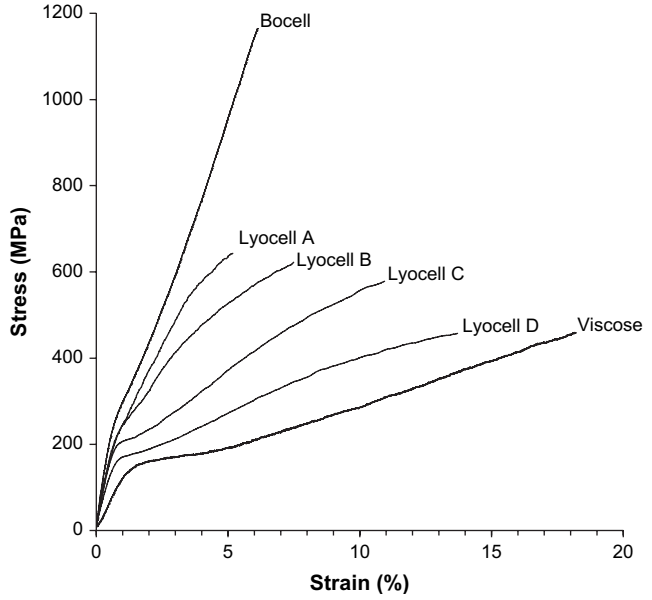

Fig. 2. Typical stress–strain curves for different regenerated cellulose fibres.

were achieved for the non-industrial Bocell fibre whereas textile viscose showed the lowest values. All four kinds of lyocell fibres tested showed an intermediate behaviour. In order to further extend the range of modulus of elasticity covered by experimental data, films of regenerated cellulose were produced and also tested in tension. The results of these tests are shown in Fig. 3 and Table 2. The strength and modulus of the cellulose films tested here is well below the values observed for fibres. Since Poisson's ratio is an input parameter required for the full description of the relationship between structure and mechanical fibre performance, it was also determined using electronic laser speckle interferometry for two-dimensional strain measurement. The resulting Poisson's ratio

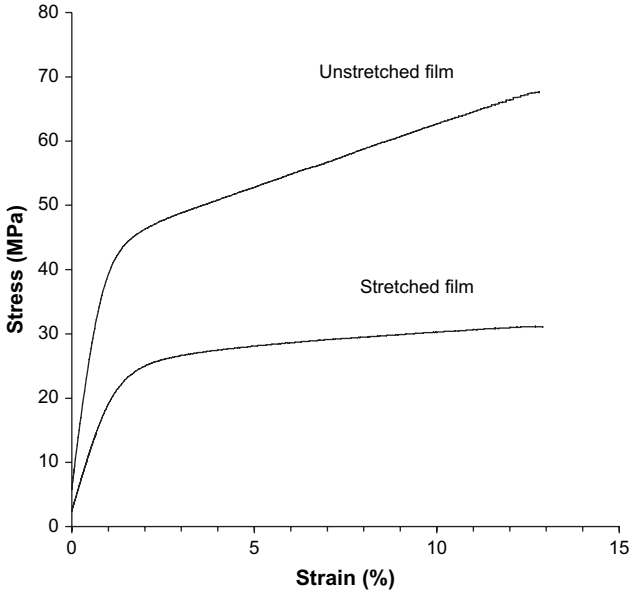

Fig. 3. Stress–strain curves for an unstretched regenerated cellulose film and for a film stretched to 50%, tested transverse to the direction of stretching.

obtained from measurements on six unstretched regenerated cellulose films was 0.30 ± 0.015.

3.3. Mechanical properties by nanoindentation

A direct measurement of the modulus of elasticity in fibre direction and transverse to the fibre direction was performed by means of nanoindentation. Fig. 4 shows an AFM image of the cross-section of a single regenerated cellulose fibre (lyocell) before and after a nanoindentation experiment. The average roughness of the surface of the fibres was very smooth with (between 1 mm and 2 nm) and well below the size of the indents. Two typical load–depth curves from a nanoindentation experiment (Fig. 5) demonstrate that there is a clear difference in the mechanical properties parallel and transverse to the fibre direction, respectively. An evaluation of load–depth curves according to the Oliver and Pharr method [26] yielded average elastic moduli shown in Table 1.

3.4. Analysis of experimental data

In this section, a simple, purely empirical model is developed, which allows making an estimate of the anisotropy of regenerated cellulose fibres based on their degree of preferred orientation expressed by birefringence. A mathematical function of the form

$$E = a + b \times e^{(c \times \Delta n)} \quad (4)$$

was used and the parameters a, b, and c were determined by least squares fitting. The result of the fitting procedure is shown in Fig. 6. As a result of the fit, the longitudinal modulus of a regenerated cellulose fibre can be estimated from its birefringence by means of Eq. (5)

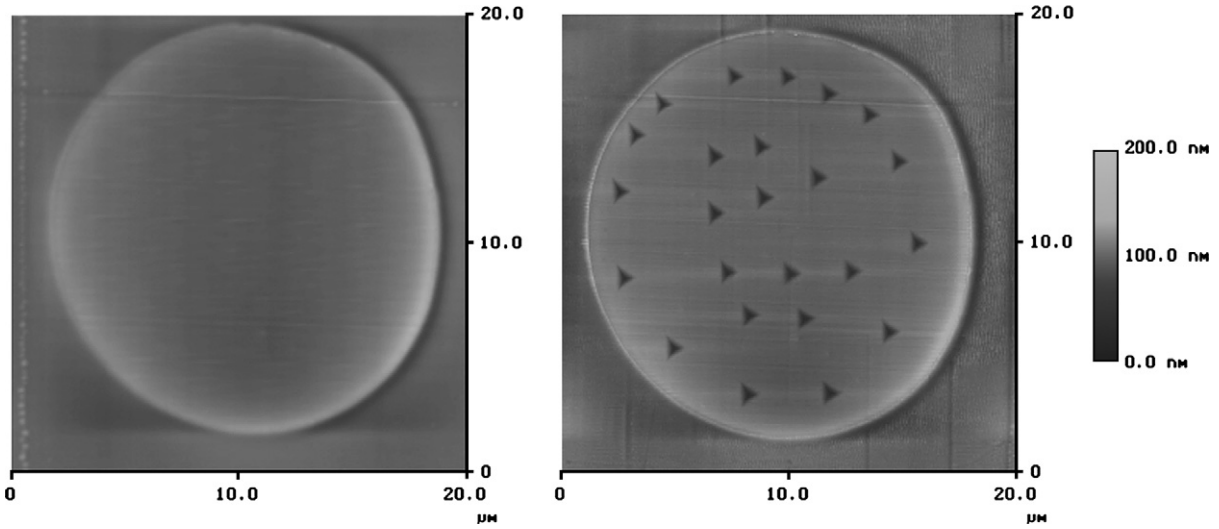

Fig. 4. AFM images of a lyocell fibre before (left) and after (right) a nanoindentation experiment. The grey scale indicates image height.

$$E = 2.8343 + 2.9184 \times e^{(49.4404 \times \Delta n)}. \quad (5)$$

Since the sign of birefringence will change when the axis of reference is rotated by 90°, the corresponding transverse modulus can be estimated from the birefringence value used for the calculation of the longitudinal modulus multiplied by −1. Results are shown in Table 3.

More results can be derived from the experimental data on birefringence and modulus of elasticity by assuming that the value of 88 GPa for the modulus of the cellulose II crystal measured by Nishino et al. [28] is correct. This enables the use of the value of 0.0615 for Δn_{max} derived in Fig. 1 for the calculation of Hermans' orientation factor f for further analysis. A plot showing the dependence of the measured tensile modulus and also the elastic moduli inferred from nanoindentation on the degree of molecular orientation expressed by Hermans' orientation factor is shown in Fig. 7. When Eq. (5) is extrapolated to $f = 1$ and $f = -1$, the modulus of elasticity at perfect longitudinal and perfect transverse orientations can be derived. For the fibres characterised in the present study, $E_{(f=1)} = 63.9$ GPa and $E_{(f=-1)} = 2.9$ GPa. The macroscopic shear modulus G of regenerated cellulose can be derived according to Eq. (6) for isotropic samples

$$G = \frac{E}{2(1+\nu)} \quad (6)$$

where ν is the macroscopic Poisson's ratio. The material closest to isotropy characterised in the present study is the

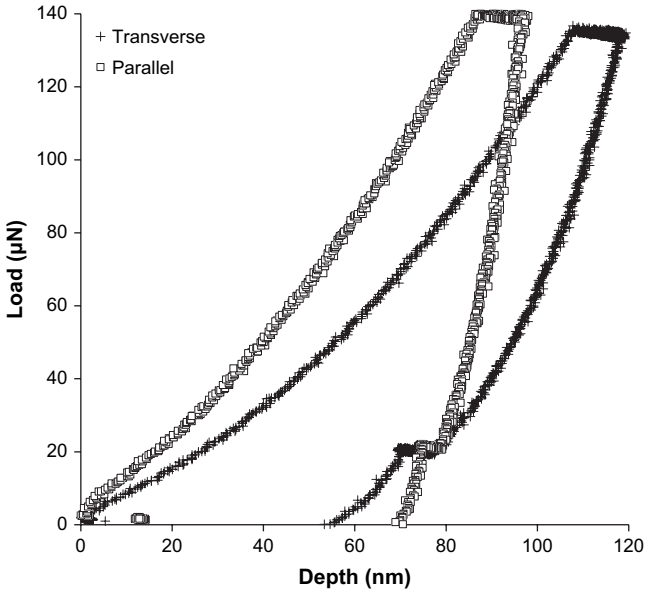

Fig. 5. Typical load–depth curves for nanoindentation experiments with cellulose fibres parallel and transverse to the fibre direction.

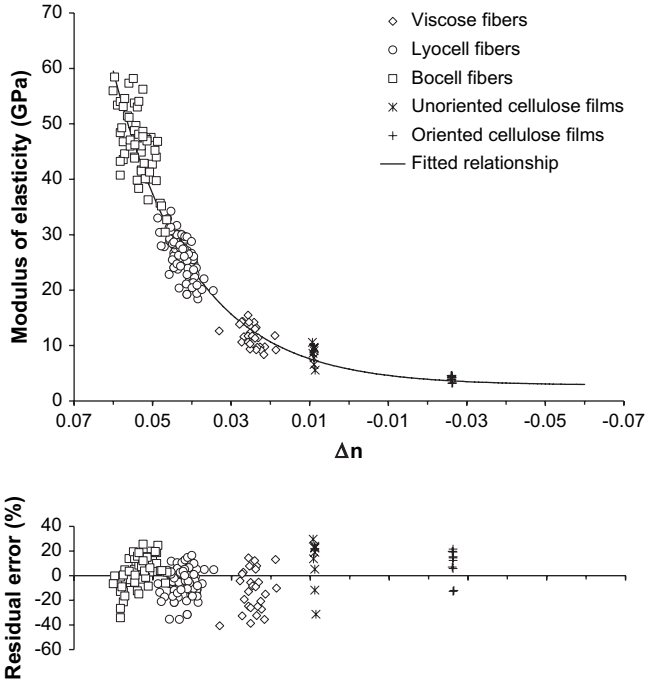

Fig. 6. Plot of the modulus of elasticity of various cellulose fibres and films against their birefringence with fit of Eq. (4) and residual error of the fit.

Table 3
Anisotropy A of the modulus of elasticity in different regenerated cellulose fibres

Fibre	A_{NI}	$A_{Eq.\ (5)}$
Bocell	2.7	15.3
Lyocell A	3.6	9.9
Lyocell B	3.6	9.6
Lyocell C	2.9	8.6
Lyocell D	2.4	6.9
Viscose	1.5	3.1

A_{NI}: ratio of the modulus of elasticity in fibre direction and transverse to the fibre direction measured by nanoindentation; $A_{Eq.\ (5)}$: ratio of the moduli obtained by dividing the longitudinal modulus of elasticity measured in tensile testing by the transverse modulus estimated from Eq. (5).

unstretched regenerated cellulose film, which was also used for the determination of the macroscopic Poisson's ratio. For this film, a macroscopic shear modulus G of 3.3 GPa is obtained. A different approach is applicable to the determination of g, the average shear modulus between adjacent cellulose chains, for well-oriented cellulose fibres [29]. In a plot of E^{-1} versus Δn the ratio of the slope and the intercept of the curve with the Δn axis is given by

$$\frac{\text{slope}}{\text{intercept}} = \frac{3g}{1+\frac{3g}{e_c}} \tag{7}$$

Such an analysis was performed individually for Bocell fibres, lyocell and viscose, assuming again a value of 88 GPa for e_c. The resulting values for g are 3.6 GPa for Bocell, 2.0 GPa for lyocell, and 0.8 GPa for viscose. Using the latter values, the relationship between molecular orientation and the macroscopic modulus of elasticity of well-oriented cellulose fibres can be described by Eq. (8) [29]

$$\frac{1}{E} = \frac{1}{e_c} + \frac{1}{3g}\left(1 - \frac{\Delta n}{\Delta n_{max}}\right). \tag{8}$$

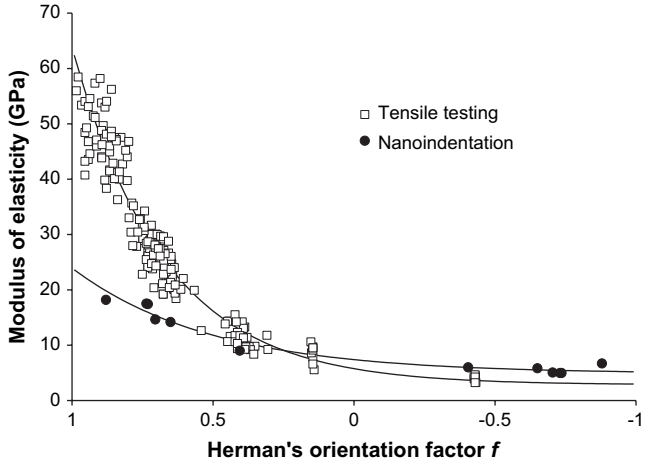

Fig. 7. Plot of the modulus of elasticity of various cellulose fibres and films measured by tensile testing against Hermans' orientation factor f compared to the corresponding moduli obtained from nanoindentation. Both data series were fitted with Eq. (4).

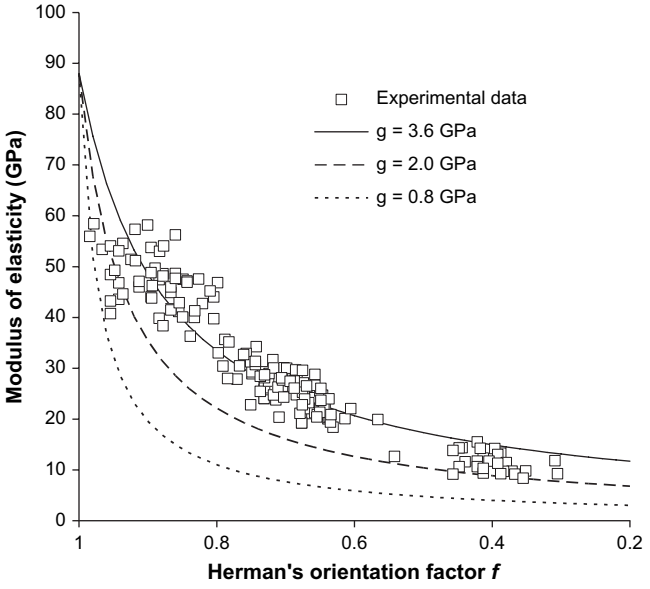

Fig. 8. Plot of the modulus of elasticity of various cellulose fibres measured by tensile testing against Hermans' orientation factor f compared to the corresponding moduli obtained from Eq. (8) with $e_c = 88$ GPa.

Results shown in Fig. 8 indicate a good fit of experimental data only with the highest value of g derived from Bocell fibres.

4. Discussion

4.1. Molecular orientation

The determination of the average molecular orientation, i.e. the choice of the correct value of maximum birefringence for cellulose, is a critical aspect in studies relating orientation derived from birefringence with mechanical properties. In the literature, different values ranging from 0.0545 [20] to 0.062 [14] and 0.081 [21] can be found. The value of 0.0545 derived from measurements with high-modulus fibres spun from phosphoric acid solution [20] was considered unsuitable for the data obtained in the present study, as it lead to physically impossible values (>1) for the Hermans' orientation factor f in many cases. By contrast, use of the rather high value of 0.081 recently published by Kong and Eichhorn [21] would require the chain modulus g of cellulose II to be more than 180 GPa in order to fit our experimental data as shown in Fig. 8, which is a highly improbable value considering the literature [15,30]. Since the maximum birefringence of 0.0615 determined in the present study agrees very well with the value of 0.062 published by Lenz et al. [14], it was presumed suitable for further analysis.

4.2. Fibre anisotropy calculated from orientation measurements and tensile tests

By means of simple models such as the one shown in Eq. (1), the relationship between molecular orientation and the modulus of elasticity of well-oriented regenerated cellulose

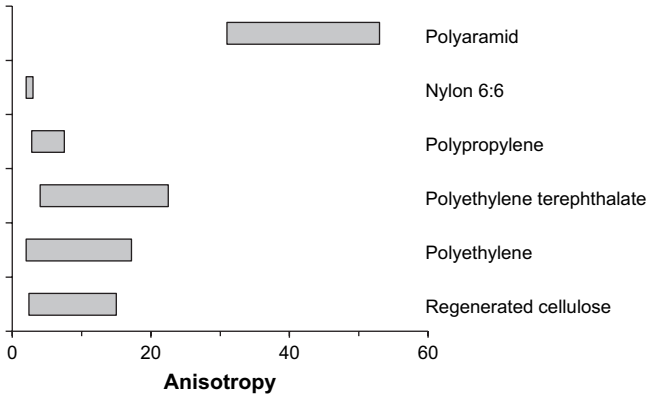

Fig. 9. The range of anisotropy (ratio between the modulus of elasticity parallel and transverse to the fibre direction) of different polymer fibres compared to regenerated cellulose fibres.

fibres can be described when the elastic and shear moduli at the level of the cellulose chain (e_c and g) are known [29]. Since there should be no difference in the modulus of elasticity of perfectly straight and parallel aligned noncrystalline cellulose macromolecules and cellulose crystallites [14], crystallinity is not considered here. Furthermore, it is also necessary to find a reasonable relation between the orientation parameter $\langle \sin^2 \theta \rangle$ determined from birefringence and the strain orientation parameter $\langle \sin^2 \Phi \rangle_E$. A comprehensive discussion on the various assumptions involved in finding such estimates is given in Ref. [20]. With respect to constitutive models such as Eq. (1), the empirical procedure chosen here has the advantage of relying solely on directly measured data (E and Δn). Also, the empirical relation derived here is applicable to the full range of possible Hermans' orientation factors, which is not the case for Eq. (1).

The calculated anisotropy of regenerated cellulose fibres characterised in the present study ranges from 3.1 for textile viscose up to 15.3 for the experimental Bocell fibre (Table 3). Using a range of different devices, the transverse modulus of various polymer fibres was measured and compared to the longitudinal modulus [31–36]. In Fig. 9 the range of anisotropy observed in a number of polymer fibres is compared to the anisotropy calculated for different regenerated cellulose fibres in the present study. It can be seen that regenerated cellulose behaves quite similar to other polymer fibres, with the notable exception of polyaramid, which shows much higher anisotropy.

In addition to fibre anisotropy, estimates for a number of macroscopic and microscopic material parameters were inferred from the experimental data measured in the present study. On the macroscopic scale, the shear modulus G and the modulus of elasticity E at perfect orientation parallel and transverse, respectively, to the fibre axis were calculated. The value of 63.9 GPa found for perfect orientation parallel to the fibre axis ($E_{(f=1)}$) should theoretically be equal to the modulus of the cellulose II chain of 88 GPa [28]. The disagreement found with present data may be due to the fact that a static modulus with fixed gage length was determined here as opposed to sonic modulus measurements, which give higher values in modulus [20]. In addition to the longitudinal modulus at perfectly parallel orientation, a value of 2.9 GPa was calculated for the expected modulus at perfect transverse orientation ($E_{(f=-1)}$). This leads to a maximum possible anisotropy for cellulose fibres of 22 when characterised by static tensile tests as performed in the present study. Disregarding potential inaccuracies in the estimation of $E_{(f=-1)}$ discussed for $E_{(f=1)}$ it can be assumed that $E_{(f=-1)} = 2.9$ GPa is equal to the average transverse modulus of elasticity of the cellulose chain. This value is to be considered an average value, since it does not take into account the different mechanical behaviour of cellulose in the transverse directions in the plane – and normal to the plane of the glucopyranose ring. The estimated anisotropy of the cellulose II chain can consequently be calculated from 88 GPa/2.9 GPa, which gives 30.

Finally, values of 3.6 GPa (Bocell), 2.0 GPa (lyocell), and 0.8 GPa (viscose) were found for the average shear modulus between adjacent cellulose II chains. According to Ref. [20], g changes independent of the degree of orientation of cellulose bonding due to different degrees of hydrogen bonding. The value for g obtained in the present study lies close to the range of values from 1.8 GPa for textile viscose to 3.8 GPa for the Bocell fibre published by Northolt et al. [20]. Furthermore, a value of 3.6 GPa derived from an analysis of a number of different lyocell fibres [21] is also reasonably close to the value found in this study, considering that fibres with different orientation were used.

4.3. Fibre anisotropy calculated from nanoindentation measurements

As shown in Table 1 there is great discrepancy between the longitudinal modulus of elasticity measured by tensile tests and the modulus measured by nanoindentation. The difference is small for the low-modulus viscose fibre, but increases significantly with increasing fibre stiffness. While the longitudinal modulus of elasticity is severely underestimated by nanoindentation, the contrary holds true for the transverse modulus, which is overestimated in general, when compared to values expected according to the fit shown in Fig. 7. Consequently, also the degree of anisotropy of the cellulose fibres tested here is underestimated when derived from nanoindentation results (Table 3). From theoretical calculations and experiments with a variety of different materials [37–40], it is well known that in nanoindentation experiments with anisotropic materials the higher modulus tends to be underestimated while the lower modulus is overestimated. This phenomenon is attributed to the fact that, due to the inclination of the flanks of the indenter body with respect to the principal material axes of the sample to be characterised, the measured apparent modulus is affected by the moduli along all material axes due to the multiaxial stress state under the indenter. For the regenerated cellulose fibres as characterised in the present study, the tensile modulus corresponding to the respective value measured by nanoindentation can be estimated from Fig. 10. Currently, there is no general solution available for the discrepancy between tensile modulus and nanoindentation modulus, but efforts are being undertaken

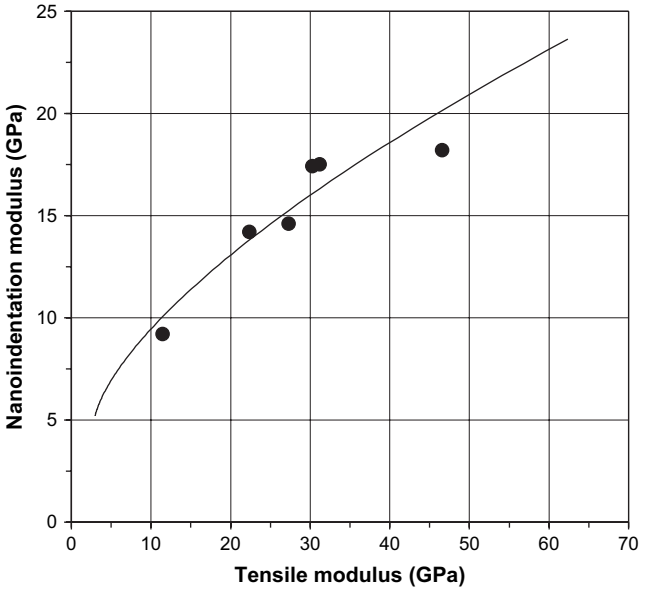

Fig. 10. Relationship between the modulus of elasticity measured by tensile testing and nanoindentation. The trendline is based on the fit to experimental data based on Eq. (4) shown in Fig. 7.

in, among others, the laboratory of the authors. It is expected that a uniaxial stress state allowing the calculation of a correct value for the modulus of elasticity will build up under a flat indenter body (''flat punch''). First prototype flat punch indenters have been produced by means of a focussed ion beam station, but more development is necessary at this state.

In spite of the fact that correct measurements of the elastic modulus of regenerated cellulose fibres could not be taken with the Berkovich indenter used in the current study, results achieved with the indenter are still very useful since they indicate that the transverse modulus of elasticity of different cellulose fibres calculated using the fit shown in Fig. 7 is most probably in the correct order of magnitude.

5. Concluding remarks

By combining results from tensile tests and birefringence measurements it was shown in the present study that it is possible to describe the relationship between the degree of preferred molecular orientation of a variety of regenerated cellulose fibres and the modulus of elasticity in the direction of the fibre, and the ratio between this modulus and the modulus transverse to the fibre using a simple empirical model. Using the model and parameters presented here, an estimate of the anisotropy of a given regenerated cellulose fibre can be made from only one input parameter, i.e. the degree of preferred orientation expressed by birefringence. Direct measurement of fibre anisotropy was also attempted by means of nanoindentation. However, the results of these measurements show that with the indenter geometry used in the present study it is not possible to obtain accurate values for the elastic moduli of cellulose fibres. We conclude that similar to other anisotropic materials, there is a discrepancy between the true modulus and the apparent nanoindentation modulus due to the inclination of the indenter pyramid with regard to the principal material axes.

References

[1] Woodings C. Regenerated cellulose fibres. Cambridge: Woodhead Publishing; 2001.
[2] Bledzki AK, Gassan J. Prog Polym Sci 1999;24:221–74.
[3] Amash A, Zugenmaier P. Polymer 2000;41:1589–96.
[4] Seavey KC, Ghosh I, Davis RM, Glasser WG. Cellulose 2001;8:149–59.
[5] Ganster J, Fink HP. Cellulose 2006;13:271–80.
[6] Ganster J, Fink HP, Pinnow M. Compos A 2006;37:1796–804.
[7] Adusumali RB, Reifferscheid M, Weber H, Roeder T, Sixta H, Gindl W. Macromol Symp 2006;244:119–25.
[8] Shindo A, Nakanishi Y, Soma I. Appl Polym Symp 1968;9:271–84.
[9] Plaisantin H, Pailler R, Guette A, Daude G, Petraud M, Barbe B, et al. Compos Sci Technol 2001;61:2063–8.
[10] Wu QL, Pan D. Text Res J 2002;72:405–10.
[11] Peng SJ, Shao HL, Hu XC. J Appl Polym Sci 2003;90:1941–7.
[12] Hermans PH, Weidinger A. J Polym Sci 1954;14:405–7.
[13] Kratky O, Sembach H. Angew Chem Int Ed Engl 1955;67:603–6.
[14] Lenz J, Schurz J, Wrentschur E. Holzforschung 1994;48(Suppl):72–6.
[15] Fink HP, Weigel P, Purz HJ, Ganster J. Prog Polym Sci 2001;26:1473–524.
[16] Eichhorn SJ, Young RJ, Davies RJ, Riekel C. Polymer 2003;44:5901–8.
[17] Northolt MG. Polymer 1980;21:1199–204.
[18] Northolt MG, van der Hout R. Polymer 1985;6:310–6.
[19] Bower DI. J Polym Sci Part B Polym Phys 1981;19:93–107.
[20] Northolt MG, Boerstoel H, Maatman H, Huisman R, Veurink J, Elzerman H. Polymer 2001;42:8249–64.
[21] Kong K, Eichhorn SJ. Polymer 2005;46:6380–90.
[22] Gindl W, Martinschitz KJ, Boesecke P, Keckes J. Biomacromolecules 2006;7:3146–50.
[23] Nakamura K, Wada M, Kuga S, Okano T. J Polym Sci Part B Polym Phys 2004;42:1206–11.
[24] Konnerth J, Gindl W, Müller U. J Appl Polym Sci 2007;103:3936–9.
[25] Adusumalli RB, Müller U, Weber H, Roeder T, Sixta H, Gindl W. Macromol Symp 2006;244:83–8.
[26] Oliver WC, Pharr GM. J Mater Res 1992;7:1564–83.
[27] Northolt MG. Lenzing Ber 1985;59:71–7.
[28] Nishino T, Takano K, Nakamae K. J Polym Sci Part B Polym Phys 1995;33:1647–51.
[29] Northolt MG, de Vries H. Angew Makromol Chem 1985;133:183–203.
[30] Northolt MG, den Decker P, Picken SJ, Baltussen JJM, Schlatmann R. Adv Polym Sci 2005;178:1–108.
[31] Hadley DW, Ward IM, Ward J. Proc R Soc London Ser A 1965;285:275–86.
[32] Pinnock PR, Ward IM, Wolfe JM. Proc R Soc London Ser A 1966;291:267–78.
[33] Phoenix SL, Skelton J. Text Res J 1974;44:934–40.
[34] Hine PJ, Ward IM. J Mater Sci 1996;31:371–9.
[35] Singletary J. Mech Compos Mater 2000;36:319–26.
[36] Stamoulis G, Wagner-Kocher C, Renner M. Exp Tech 2005;29:26–31.
[37] Vlassak JJ, Nix WD. Philos Mag A 1993;67:1045–56.
[38] Vlassak JJ, Nix WD. J Mech Phys Solids 1994;42:1223–45.
[39] Swadener JG, Rho JY, Pharr GM. J Biomed Mater Res 2001;57:108–12.
[40] Gindl W, Schöberl T. Compos A 2004;35:1345–9.